THE INTERNATIONAL RESEARCH INSTITUTE FOR CLIMATE PREDICTION
LINKING SCIENCE TO SOCIETY

IRI TECHNICAL REPORT NO. 02-05

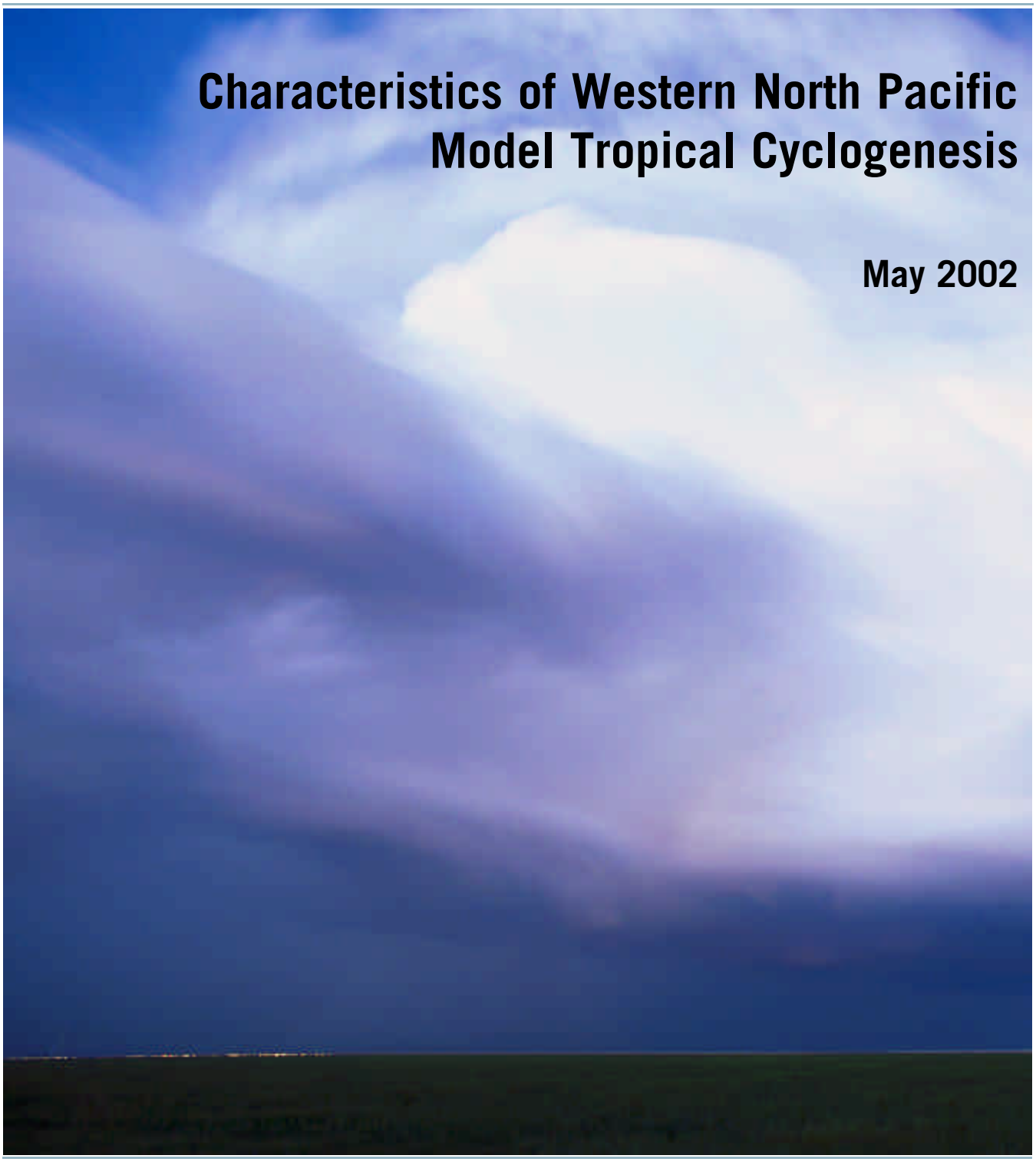

Characteristics of Western North Pacific Model Tropical Cyclogenesis

May 2002

COLUMBIA EARTH INSTITUTE
COLUMBIA UNIVERSITY IN THE CITY OF NEW YORK

Characteristics of Western North Pacific Model Tropical Cyclogenesis

SUZANA J. CAMARGO *
International Research Institute for Climate Prediction,
Lamont-Doherty Earth Observatory of Columbia University, Palisades, NY
and
ADAM H. SOBEL
Department of Applied Physics and Applied Mathematics,
Department of Earth and Environmental Sciences,
Columbia University, New York, NY

*IRI, Lamont-Doherty Earth Observatory of Columbia University, 61 Route 9W, PO Box 1000, Palisades, NY 10964-8000, *email*:suzana@iri.columbia.edu

Abstract

"Tropical cyclogenesis" in a low-resolution Atmospheric General Circulation model is studied, focusing on the Western North Pacific region during the June-October typhoon season. Time-dependent composites of the cyclones are formed and analyzed, with a focus on the temporal evolution of quantities averaged in space around the storm centers. Day zero of each composite corresponds to the time at which the cyclone passes the criteria for detection.

Some variables whose magnitude is related to cyclone intensity (such as low-level vorticity and surface wind speed) show similar temporal evolution, with a slight decrease up to a few days before day zero, a weak local minimum at that point, and a strong increase after that for a week or more. The relative humidity at low levels has its minimum somewhat later, at about day zero. The mean composite environmental vertical wind shear lacks a minimum and increases monotonically through the entire genesis period until a week after day zero. This variation is mostly due to the mean cyclone track's moving through regions of different climatological shear, which varies monotonically from easterly to westerly, crossing zero shortly after day zero, and would be consistent with a controlling role of the shear on model cyclogenesis. A signal in the skewness of the lower-level relative humidity distribution over the ensemble suggests that a dry lower troposphere can prevent development of a model cyclone.

The local minimum in many variables' time series suggests the presence of an initial disturbance that is suddenly enhanced, becoming a model tropical cyclone, as has been noted in observations.

1. Introduction

Storms having gross features similar to tropical cyclones have long been observed in Atmospheric General Circulation Models (GCMs) (Manabe et al., 1970), although the intensity is much lower and spatial scale much larger in the simulated storms than in observed tropical cyclones (Bengtsson et al., 1982; Vitart et al., 1997). The climatology and structure of these model cyclones has been studied (Bengtsson et al., 1982, 1995), as have their interannual variability and relation to El Niño-Southern Oscillation (ENSO) (Wu and Lau, 1992). More recently, Vitart et al. (1997) studied tropical cyclones in GCMs using an ensemble of integrations and explored their relation to the large scale circulation (Vitart et al., 1999) and sea surface temperature variability (Vitart and Anderson, 2001). Studies of global cyclogenesis using global high resolution models have also been performed, for limited time periods (Krishnamurti and Oosterhof, 1989; Chan and Kwok, 1999).

Seasonal forecasts of tropical cyclone activity for some ocean basins are produced using statistical methods applied to observations, e.g. Gray et al. (1993); Nicholls (1992); Chan et al. (1998). GCMs can also be used to make dynamical seasonal forecasts of tropical cyclone activity (Bengtsson, 2001). Dynamical forecasting of seasonal tropical storm activity are produced at ECMWF (European Centre for Medium-Range Weather Forecasts) based on coupled ocean-atmosphere models (Vitart and Stockdale, 2001). One method uses the GCM to predict large-scale variables which affect tropical cyclone activity (Ryan et al., 1992; Watterson et al., 1995; Thorncroft and Pytharoulis, 2001). Another method involves detecting and tracking the "tropical cyclones"[1] in the model itself, and then basing the prediction on the statistics of those storms (Manabe et al., 1970; Bengtsson et al., 1982; Krishnamurti, 1988; Krishnamurti et al., 1989; Broccoli and Manabe, 1990; Wu and Lau, 1992; Haarsma et al., 1993; Bengtsson et al., 1995; Tsutsui and Kasahara, 1996; Vitart et al., 1997; Vitart and Stockdale, 2001). Despite the low intensity and large spatial scale of the model storms, their spatial and temporal distributions are similar to those of observed storms (Bengtsson et al., 1995; Vitart et al., 1997), suggesting that this approach has some chance of success. To the extent that this method of seasonal forecasting assumes some confidence in the model's ability to produce storms in (statistically) the right places and times for the right reasons, it behooves us to obtain a better understanding of the cyclogenesis process in the GCM.

Western North Pacific model tropical storms are studied here using a 13-member ensemble of low-resolution ECHAM4.5 GCM (Roeckner et al., 1996) simulations forced by observed sea surface temperature in the period 1979–1995. Tropical storms are detected by a basin and model-dependent algorithm incorporating multiple physical fields, and then tracked using the low-level vorticity (Camargo and Zebiak, 2002a). In this paper time-dependent composites of model tropical cyclones are analyzed. Our broad aim is to understand the physical processes controlling tropical cyclogenesis in the model. Here we take a first step towards this understanding by documenting some basic features of the typical model cyclogenesis, and making a few preliminary comments on their similarities and differences with respect to what is known about observed tropical cyclogenesis. Using an ensemble of model integrations gives us a large statistical sample and therefore, hopefully, robust features in the composites.

The general features of the model tropical cyclones in the Western North Pacific and the com-

[1]Hereafter, we drop the quotes around the term, but they should be considered implicit due to the substantial differences between the simulated storms and observed tropical cyclones.

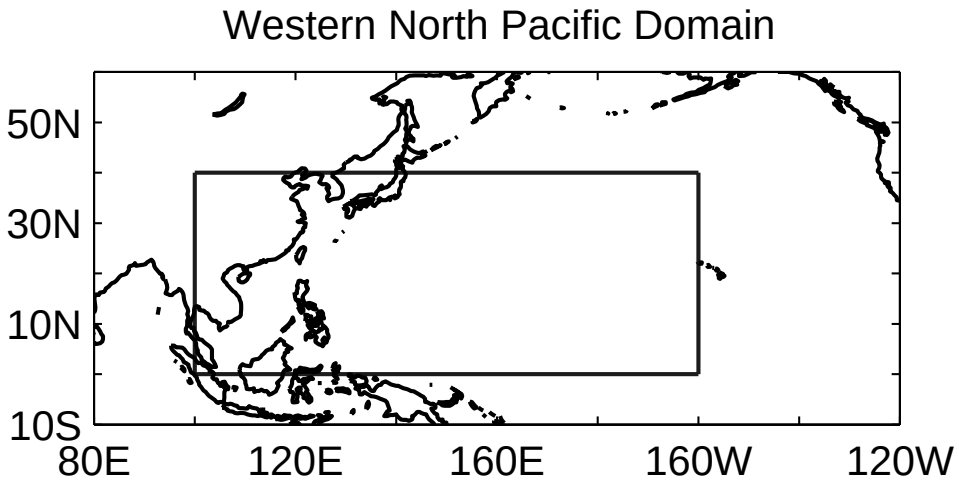

Figure 1: Definition of the Western North Pacific basin domain used in this study.

positing technique are described in Section 2. The characteristics of the composites and our main results are given in Section 3, and we conclude in Section 4.

2. Time Composites of Western North Pacific Model Tropical Cyclones

This study uses model data from a 13-member ensemble of ECHAM4.5 (Roeckner et al., 1996) simulations using T42 resolution and observed monthly mean sea surface temperatures for the period 1979–1995. Tropical cyclones are detected and tracked globally using basin and model-dependent algorithms described in Camargo and Zebiak (2002a). The algorithm has two parts. In the detection part, cyclones that meet environmental and duration criteria are identified. In the tracking part, cyclone tracks are obtained from the vorticity centroid and relaxed criteria. Only tropical cyclones that form in the Western North Pacific Basin region shown in Fig. 1 are considered.

A reason for selecting this region is that the annual cycle of tropical cyclone frequency produced by the model in the Western North Pacific is very similar to that observed (Camargo and Zebiak, 2002b). Observed interannual variability of tropical cyclone activity in the Western North Pacific basin is fairly small, and the model has low skill at predicting this variability. More interannual variability is observed when sub-regions of the Western Pacific basin are considered separately. The model has significant skill in simulating cyclone frequency interannual variability in the middle of the basin where ENSO influence is strong (Camargo and Zebiak, 2002b). According to ENSO phase, the average genesis location of model cyclones exhibits a northwest-southeast shift (Camargo and Zebiak, 2002b), similar to that observed (Lander, 1994). Compared to observed cyclones, fewer model cyclones curve around the continent as they move poleward and reach high latitudes (Camargo and Zebiak, 2002a).

Time-dependent composites of Western North Pacific model tropical storms use model cyclones from the June-October typhoon season; the 13-member ensemble simulation produces a total of 5701 cyclones in the period 1979-1995. Composites are created by averaging simulated

fields from different storms in a storm-centered coordinate. Storms are aligned on the first day they pass the detection criteria (here called day 0) and extend backward and forward for 15 days 0; while all storms are included on day 0, not all storms can be tracked 15 days before and after their passing the detection criteria. In addition to composite means, extreme values (maximum and minimum), standard deviation and skewness among all storms used in the composite were analyzed. Composites were formed in an area around the center of each storm of size 7×7 grid boxes corresponding to a square box with sides of approximately 16.8 degrees.

When computing composite quantities, it is useful to have some way of quantifying how strongly the various quantities are perturbed by the existence of a tropical cyclone in the model. For understanding tropical cyclogenesis, a method which has been useful in analyzing observations has been to identify precursor disturbances which appear likely to intensify into tropical cyclones, and then classify those as "developing" or "non-developing" according to whether they do in fact undergo genesis (McBride, 1981a; McBride and Zehr, 1981; McBride, 1981b; Zehr, 1992). Here, even the mature disturbances are sufficiently weak that such a distinction is not practical in that a "non-developing" storm would be barely distinguishable from the background model variability. Therefore, we simply define anomalies for each storm relative to monthly mean model climatology for the date and location of that storm, and then these anomalies are averaged over all storms to produce time series of anomalous fields.

3. Results

The tropical cyclone signal was clearly present in all model variables that were composited. Here we present results using those variables considered important in observational studies of cyclogenesis. Horizontal maps of the composite 850hPa vorticity, surface wind-speed, precipitation and 850hPa relative humidity at day 0 are shown in Fig. 2. The largest vorticity values are found in the storm center, near the largest relative humidity values, which have a small shift to the east. The precipitation maximum occurs to the east of the storm center; the observed precipitation maximum is not symmetrical around the storm center (Frank, 1977). The surface wind-speed has two maxima around the storm center, where a local minimum of the surface wind-speed is located. The structure of the storms at day 0 justifies our choice for the storm composite size.

For the rest of this section, we examine time series of various composite quantities averaged in space around the storm centers in different pressure levels.

The time evolution of the composite mean vorticity and anomalous vorticity at $850hPa$ is shown in Fig. 3. Initially, the mean low-level vorticity is larger than the climatological value, suggesting the presence of an initial disturbance days before the tropical storm appears, similar to the description of Zehr (1992) for observed tropical cyclones. The mean low-level vorticity of the composite then has a minimum at day -3 after which it sharply increases until day 3, characterizing the transition to the model tropical storm. The anomalous vorticity has a maximum on day 7, while the mean vorticity remains constant, implying that storms usually move to a region of lower climatological (relative) vorticity. The time evolution of the vorticity at other levels of the lower troposphere is very similar, as shown in Fig. 4. At upper levels, the signal of cyclogenesis on the vorticity starts later, on day 0 and there the vorticity is negative (see Fig. 4). Observed pre-typhoon and pre-hurricane systems are located in large areas of high values of low level vorticity (McBride and Zehr, 1981).

Higher values of vorticity at upper levels occur simultaneously with a sharp decrease of the

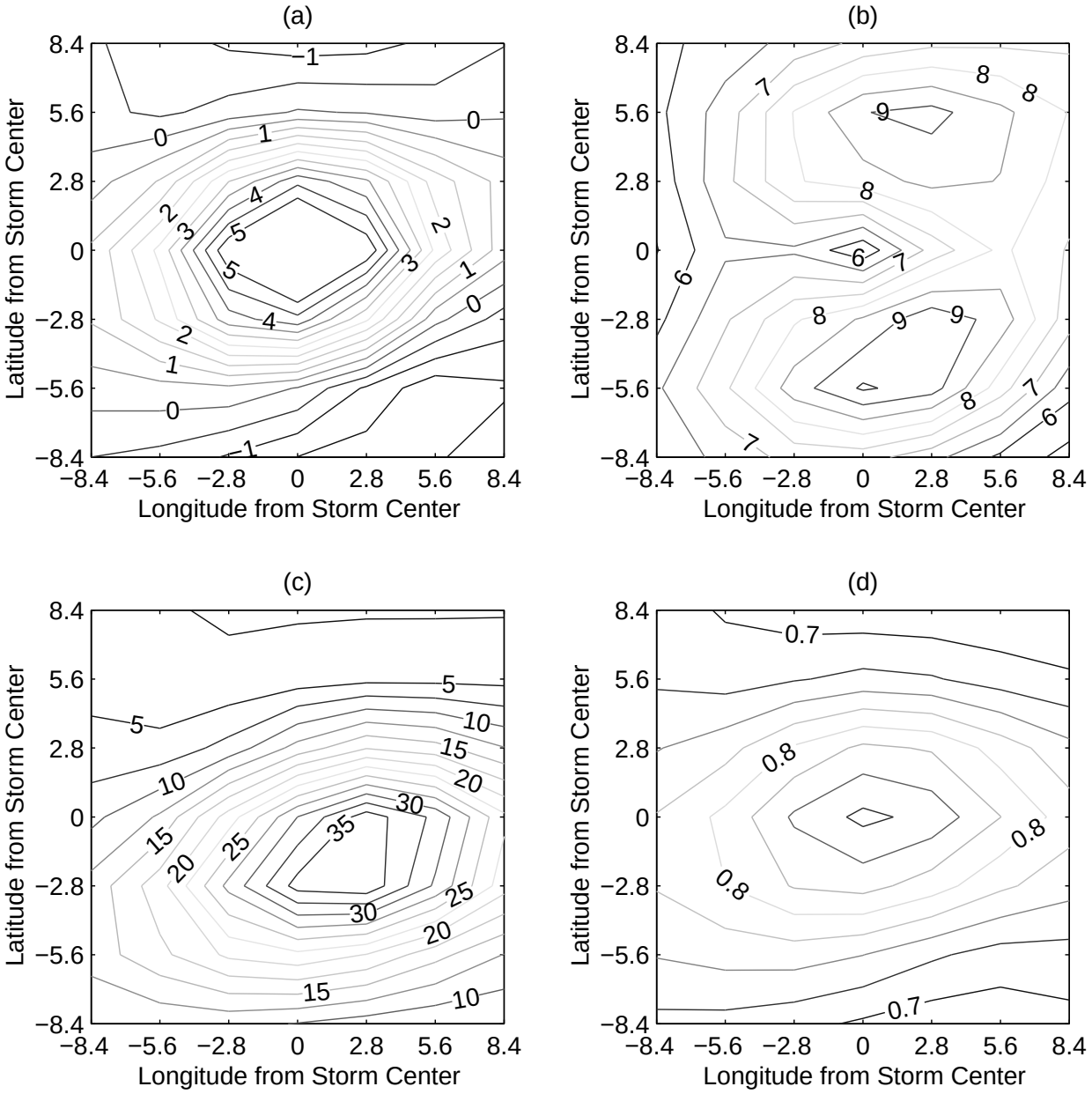

Figure 2: Contour plots of composite variables at day 0: (a) vorticity $850hPa$ ($\times 10^{-5}/s$), (b) surface windspeed (m/s), (c) precipitation (mm/day), (d) relative humidity $850hPa$.

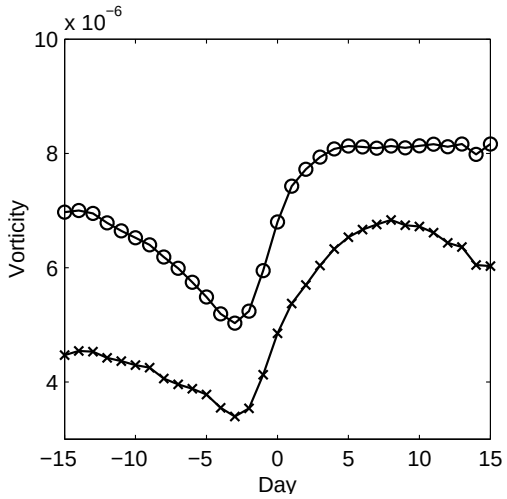

Figure 3: Composite mean vorticity ($\circ$) and anomalous vorticity ($\times$) time evolution (in $1/s$).

mean composite surface pressure (Fig. 5) and an increase of the mean composite surface windspeed (Fig. 6). The intensity of observed tropical cyclones is usually characterized by the values of the surface pressure and the surface winds. Anomalies in both these quantities, as well as in low-level vorticity, differ significantly from zero days before the model tropical cyclone is defined. The composite surface pressure anomaly has a minimum near day -15, increases until day -3, then sharply decreases. This first minimum of the surface pressure days before the genesis is analogous to the observed low in sea level pressure when pre-cyclonic cloud-clusters are formed (Lee, 1989). As the minimum of the surface pressure occurs on the edge of the period diagnosed in this study (-15 days), there is a possibility that the minimum surface pressure could even have occurred before that.

The anomalous temperature at different pressure levels is shown in Fig. 7. Similar to the low-level vorticity, the composite anomalous temperature in different levels has a minimum around day -3 and then increases abruptly reaching a maximum around day 7, while the composite mean temperature is almost constant. Model storms move to regions of lower climatogical temperatures (poleward). The largest values of mean anomalous temperature occur at upper levels and the minimum at lower levels. After day 5 the anomalous temperature at $850hPa$ begins to diminish while remaining constant at other levels. Observed composite of cloud-clusters develop in a warm atmosphere over a large horizontal scale and the warm temperature anomalies in upper levels ($300hPa$) are much more pronounced in developing than non-developing systems (McBride and Zehr, 1981).

The signals in 850 hPa vorticity, surface pressure, surface wind, and 850 hPa temperature all begin intensifying at approximately the same time, as shown by the figures. This may be viewed as different than observed tropical cyclogenesis in that in observations, a midlevel, cold-core vortex forms first and then extends downward to the surface and develops a surface warm core (e.g., Bister and Emanuel (1997)). We do not currently have an explanation for this difference.

The composite mean anomalous relative humidity (RH) for different levels is shown in Fig. 8. The anomalous RH first increases at middle levels, then at upper levels, and then only when the

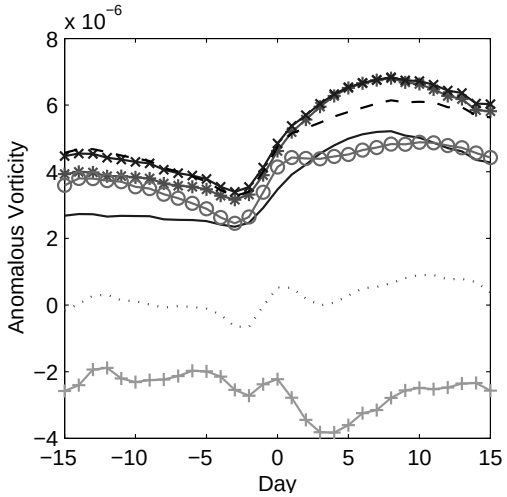

Figure 4: Composite mean anomalous vorticity time evolution at different pressure levels: $1000hPa$ (continuous line), $925hPa$ ($*$), $850hPa$ ($\times$), $700hPa$ (dashed line), $500hPa$ ($\circ$), $300hPa$ (dotted line) and $200hPa$ ($+$) (in $1/s$).

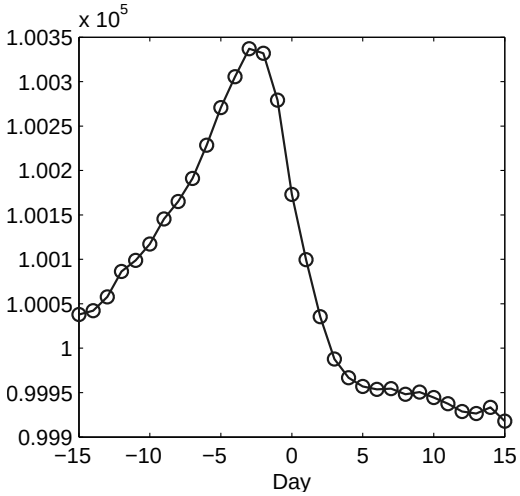

Figure 5: Composite minimum surface pressure ($\circ$) time evolution (in Pa).

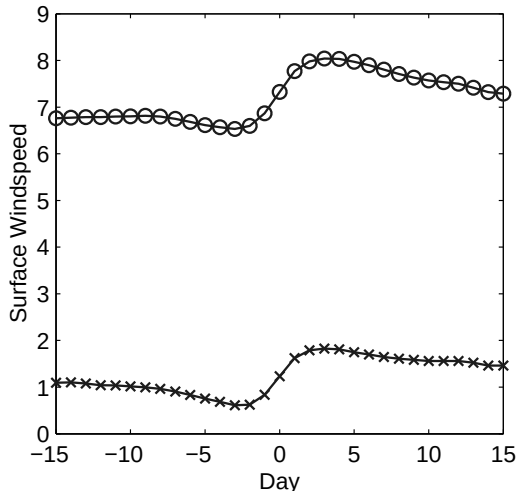

Figure 6: Composite mean surface winds ($\circ$) and anomalous surface winds ($\times$) time evolution (in m/s).

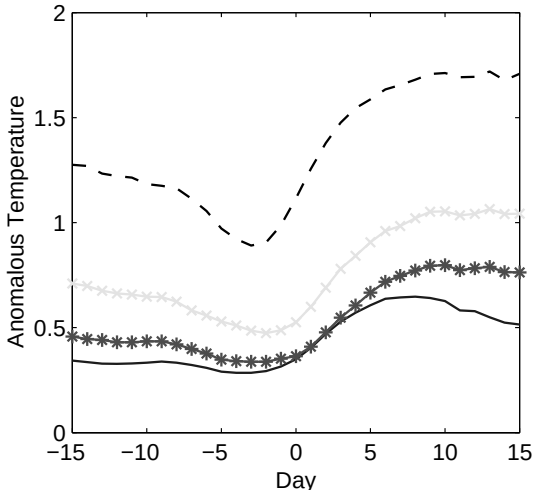

Figure 7: Composite mean anomalous temperature at differents pressure levels: $850hPa$ (continuous line), $700hPa$ ($*$), $500hPa$ ($\times$) and $300hPa$ (dashed line) (in K).

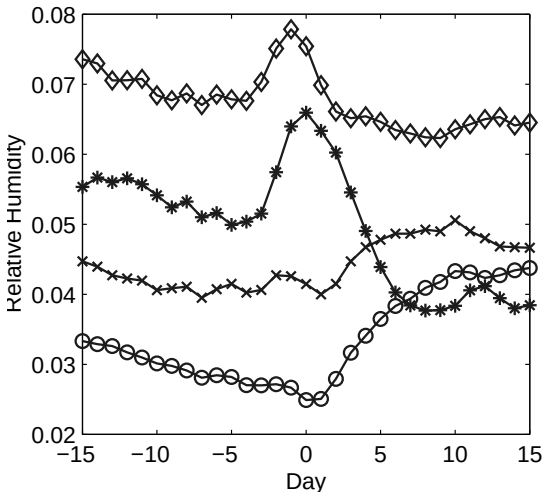

Figure 8: Time evolution of the composite mean anomalous relative humidity at 850hPa ($\circ$), 700hPa ($\times$), 500hPa ($\diamond$) and 300hPa ($\star$).

storm is well developed do the lower level RH anomalies peak. The 850 hPa RH minimum occurs around day zero, significantly later than the minima in 850 hPa vorticity and surface winds. At middle and upper levels the anomalous RH has a definite peak around day zero and then decrease sharply. The largest values of the anomalous RH occur at middle levels ($500hPa$). Lee (1989) also noticed the importance of the moistening of the middle troposphere in the formation of cloud-clusters.

A plausible explanation for this would be that a burst of convection centered on day zero (e.g., see precipitation, Fig. 12) transports low-level moisture upwards, moistening the middle and upper levels and drying the lower levels. The vortex stretching associated with this burst of convection amplifies the vorticity. Associated with this the surface winds increase, and over the following few days the associated evaporation increase moistens the lower levels. The differences between the temporal evolution of our simulated composite vortex and observed ones (e.g. Bister and Emanuel (1997)) could be due to errors, perhaps subtle ones, in how the convective parameterization both produces and responds to vertically structured humidity perturbations.

The temporal behavior of the standard deviation and skewness of different variables over the distribution of model storms was also analysed. An interesting signal is found in the skewness of the 850hPa RH. Because the mean 850hPa RH is high (around 80%), the maximum possible is 100%, we naively expect a negative skewness. The standard deviation of the RH at $850hPa$ (not shown) is approximately constant in time with a value of 5%, which is about one-fourth of the "distance" between the mean RH and the maximum of 100%. At most levels and times, a negative skewness is indeed found. However, at 850 hPa the RH skewness is positive for several days just before and through day 0, as shown in Fig. 9. This positive skewness, and its location in the time series (roughly centered on the time at which the vorticity, etc., begin increasing), suggest a constraint excluding *low* RH values from the distribution. This is consistent with the physical idea that a necessary condition for model cyclogenesis is high RH values in the lower troposphere (Gray, 1979; Rotunno and Emanuel, 1987).

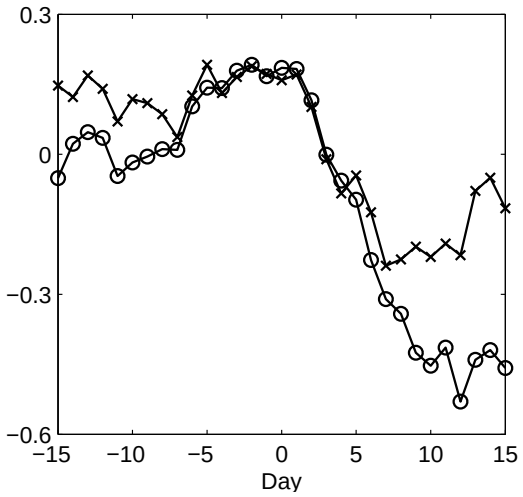

Figure 9: Time evolution of the skewness of the composite mean relative humidity ($\circ$), and of the anomalous relative humidity ($\times$) at $850hPa$.

The time series of the composite mean shear, mean anomalous shear and mean climatological shear is shown in Fig. 10; the shear is defined as the difference of the zonal velocity averaged over the compositing region at $200hPa$ and $850hPa$. The averaging is done first and then the shear computed, so it is an "environmental" shear. Unlike most other model variables the mean composite shear does not have a minimum near the time when the model storm is defined, but a week later; the mean composite shear is monotonically decreasing in absolute value through the period of genesis.

The tendency of other model variables to show similar temporal evolution, with minima a few days before day 0 and then strong increases for 10 days or so, suggests that while all these variables are indicators of storm intensity, one cannot be singled out as causally controlling the others. The very different temporal evolution of the shear, on the other hand, is consistent with, but not proof of, a causally controlling role for the shear, as has been hypothesized earlier (Gray, 1979; McBride, 1981a; McBride and Zehr, 1981; McBride, 1981b). We can imagine that as the initial disturbance begins to organize, it drifts poleward into a region of weaker shear. The similarity between the time series of composite mean and climatological shear suggests that the decrease in shear is primarily due to the mean storm trajectory from regions of higher to lower shear (easterly shear becoming less so) rather than dynamical changes in shear at a given location. We can hypothesize that if the shear reduces below a certain threshold value—3-4 $m\ s^{-1}$ is suggested by the figure—intensification occurs, while otherwise it does not, thus excluding storms which do not propagate into weak-shear regions from the composites. This would imply an important causal role for the mean shear as dynamical control on genesis.

At the same time, the tendency of the storms to move northward will produce the same time evolution of the shear even if the intensification occurs for entirely independent reasons, so from the evidence here we cannot make a conclusive judgment about the role of shear in the model cyclogenesis.

The terms in the composite anomalous net column-integrated moist static energy budget —

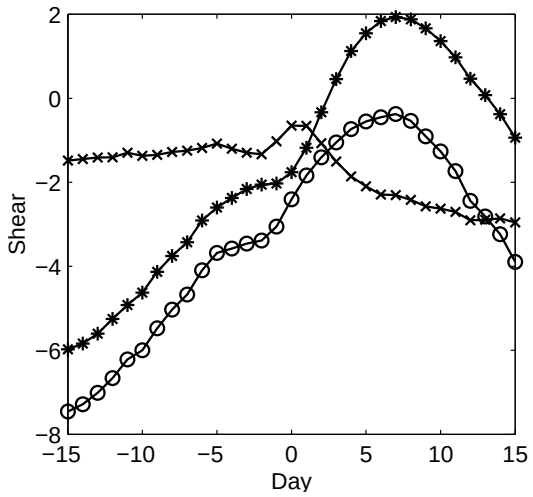

Figure 10: Time evolution of the composite mean ($\circ$), anomalous ($\times$) and climatological shear ($\star$) (in m/s).

surface sensible and latent heat fluxes at the surface, and radiative shortwave and longwave fluxes at the top of the atmosphere (TOA) — are shown in Fig. 11. TOA (a) and surface (b) fluxes are shown in separate panels and defined as positive downward. Also shown (redundantly) in each panel is the net vertical anomalous moist static energy flux convergence due to the sum of these terms. This last quantity also has a minimum on day -3 and then a sharp increase with a maximum on day 2, and is positive throughout. The tendency of column-integrated moist static energy is quite small, so that this vertical flux convergence implies a compensating horizontal export of moist static energy, as occurs in real tropical cyclones (McBride, 1981b) as well as the convective regions of larger-scale, climatic circulations (Neelin and Held, 1987). Of the model heat and radiation fluxes leading to the moist static energy flux convergence, the dominant ones are the anomalous surface latent heat flux and the anomalous outgoing longwave radiation (OLR) flux at the TOA. The shortwave flux also has anomalies comparable in magnitude to those two terms ($\sim 20-30\ W\ m^{-2}$) at both surface and TOA, although much of this is nondivergent in the atmosphere so that the anomaly in atmospheric solar absorption is closer to $10\ W\ m^{-2}$ and also has less temporal variation than the surface latent heat flux and OLR. The importance of the surface latent heat flux in the cyclogenesis process is described in theoretical (Rotunno and Emanuel, 1987) and observational (Gray, 1979) studies. The OLR signal reflects that the model is producing clouds at the location of model tropical storms, reducing the radiative cooling of the atmosphere. This apparently provides a positive feedback of comparable magnitude to the surface latent heat flux in the model, although latter is presumably underestimated due to the excessively weak surface winds in the simulated storms. The composite time series of precipitation is shown in Fig. 12, and has a temporal structure similar to that of the low-level vorticity, surface wind etc. Vertical velocity at midlevels (not shown) also has a very similar structure.

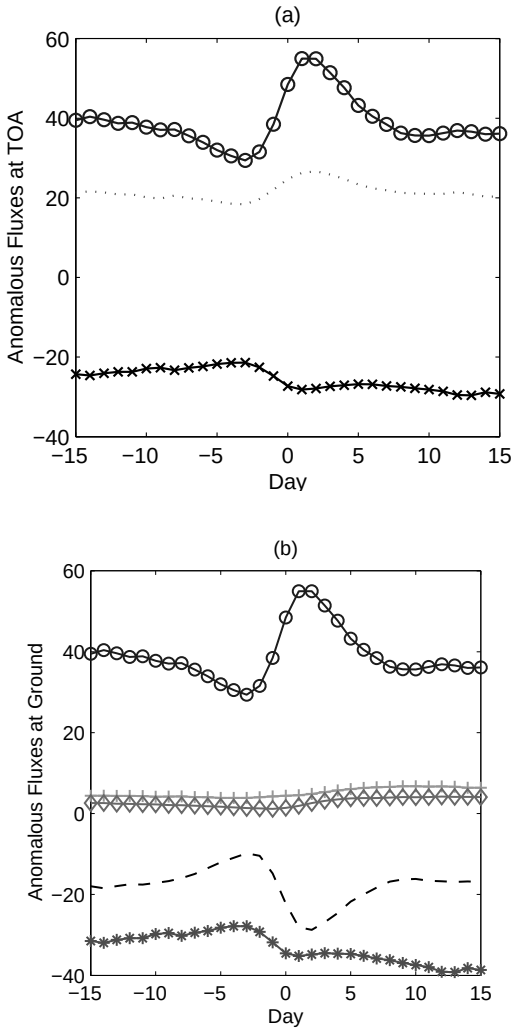

Figure 11: Time evolution of the composite mean anomalous radiation and heat fluxes magnitudes at the top of the atmosphere (TOA) (a): outgoing longwave radiation flux (dotted line), short wave flux at TOA ($\times$); and surface (b): longwave ($+$) and shortwave ($*$) fluxes at the ground, latent (dashed line) and sensible ($\diamond$) heat fluxes (in W/m^2). The moist static energy forcing ($\circ$) is shown in both panels.

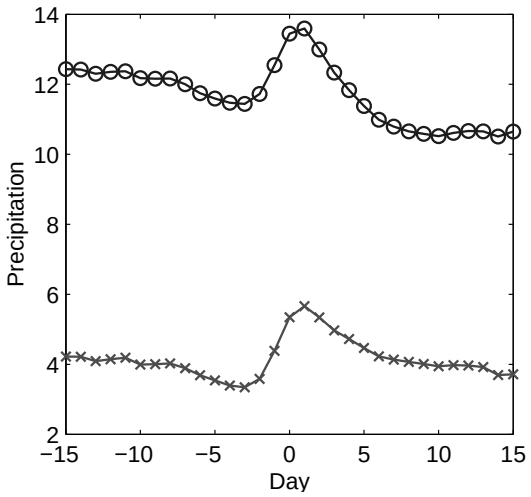

Figure 12: Time evolution of the composite mean ($\circ$), anomalous ($\times$) precipitation (mm/day).

4. Conclusions

Time-dependent composites of tropical storms on the Western Pacific are studied in a low resolution GCM. There are clear signals of the storms in all the variables that were composited. Many features of the observed genesis process resemble observations, although others (besides the obvious low intensity and large spatial scale of the storms) do not.

In most of the composite time series, a sharp increase (decrease, in the case of surface pressure) in the mean value of the variable occurs over a period of several days centered on day 0. In many of the variables, such as the low-level vorticity, surface wind, surface pressure, and precipitation, the intensification has similar temporal structure, with the minimum at approximately the same point in time. The low-level relative humidity, however, begins increasing a few days later than these other variables. The vortex structure appears to intensify simultaneously at all levels from the middle troposphere down to the surface, unlike the downward development discussed by Bister and Emanuel (1997). Broadly, however, the presence of a minimum intensity prior to development (as opposed to a pure monotonic increase throughout the composite period) is reminiscent of observed cyclogenesis as documented by Zehr (1992).

Unlike other variables, the the composite environmental wind shear varies monotonically over the storm trajectory, primarily because the mean storm trajectory moves from a region of relatively high (easterly) climatological shear to one of relatively low (and eventually, westerly) climatological shear. This is consistent with the hypothesis that weak shear is a necessary prerequisite for model cyclogenesis. However, the alternate hypothesis, that the monotonic shear decrease is coincidental and genesis occurs for entirely different reasons, cannot be ruled out.

The skewness of the 850 hPa relative humidity (RH) distribution of the ensemble of storms is generally negative, as we might naively expect due to the existence of an upper bound at 100%. However, for a period of several days centered on the minimum in other variables (thus corresponding to the beginning of the genesis period), the skewness becomes positive. Anomalously low values of RH at 850 hPa are thus excluded from the distribution particularly during this time,

suggesting that such low values inhibit storm development, i.e., that a moist lower troposphere is a prerequisite for development, as expected from observations.

Acknowledgement The authors would like to thank Max-Planck Institute for Meteorology (Hamburg, Germany) for making their model ECHAM accessible to IRI. We thank Drs. Michael K. Tippett and Stephen E. Zebiak (IRI) for their comments on this paper.

References

Bengtsson, L., 2001: Hurricane threats. *Science*, **293**, 440–441.

——, H. Böttger, and M. Kanamitsu, 1982: Simulation of hurricane-type vortices in a General Circulation Model. *Tellus*, **34**, 440–457.

——, M. Botzet, and M. Esh, 1995: Hurricane-type vortices in a General Circulation Model. *Tellus*, **47A**, 175–196.

Bister, M., and K. A. Emanuel, 1997: The genesis of hurricane Guillermo: TEXMEX analyses and a modeling study. *Mon. Wea. Rev.*, **125**, 2662–2682.

Broccoli, A. J., and S. Manabe, 1990: Can existing climate models be used to study anthropogenic changes in tropical cyclone climate? *Geophys. Rev. Lett.*, **17**, 1917–1920.

Camargo, S. J., and S. E. Zebiak, 2002a: Improving the detection and tracking of tropical storms in Atmospheric General Circulation Models. IRI Technical Report 02-02, International Research Institute for Climate Prediction, Palisades, NY, to be published in Wea. Forecasting.

——, and ——, 2002b: Variability of tropical storms in Atmospheric General Circulation Models. *Proc. of the 25th Conf. on Hurricanes and Tropical Metereology*, American Metereological Society, San Diego, CA, 148–149.

Chan, J. C. L., and R. H. F. Kwok, 1999: Tropical cyclone genesis in a global numerical weather prediction model. *Mon. Wea. Rev.*, **127**, 611–624.

——, J. E. Shi, and C. M. Lam, 1998: Seasonal forecasting of tropical cyclone activity over the Western North Pacific and the South China Sea. *Wea. Forecasting*, **13**, 997–1004.

Frank, W. M., 1977: The structure and energetics of tropical cyclone I. Storm structure. *Mon. Wea. Rev.*, **105**, 1119–1135.

Gray, W. M., 1979: *Metereology over the Tropical Oceans*, Roy. Meteor. Soc., chapter Hurricanes: Their formation, structure and likely role in the tropical circulation. 155–218.

——, C. W. Landsea, P. W. M. Jr., and K. J. Berry, 1993: Predicting Atlantic basin seasonal tropical cyclone activity by 1 August. *Wea. Forecasting*, **8**, 73–86.

Haarsma, R. J., J. F. B. Mitchell, and C. A. Senior, 1993: Tropical disturbances in a GCM. *Clim. Dyn.*, **8**, 247–257.

Krishnamurti, T. N., 1988: Some recent results on numerical weather prediction over the tropics. *Aust. Meteor. Mag.*, **36**, 141–170.

——, and D. Oosterhof, 1989: Prediction of the life cycle of a supertyphoon with a high-resolution global model. *Bull. Amer. Meteor. Soc.*, **70**, 1218–1230.

——, ——, and N. Dignon, 1989: Hurricane prediction with a high resolution global model. *Mon. Wea. Rev.*, **117**, 631–669.

Lander, M. A., 1994: An exploratory analysis of the relationship between tropical storm formation in the western north pacific and enso. *Mon. Wea. Rev.*, **122**, 636–651.

Lee, C. S., 1989: Observational analysis of tropical cyclogenesis in the Western North Pacific. Part I: Structural evolution of cloud clusters. *J. Atmos. Sci.*, **46**, 2580–2598.

Manabe, S., J. L. Holloway, and H. M. Stone, 1970: Tropical circulation in a time-integration of a global model of the atmosphere. *J. Atmos. Sci.*, **27**, 580–613.

McBride, J. L., 1981a: Observational analysis of tropical cyclone formation. Part I: Basic description of data sets. *J. Atmos. Sci.*, **38**, 1117–1131.

—, 1981b: Observational analysis of tropical cyclone formation. Part III: Budget analysis. *J. Atmos. Sci.*, **38**, 1152–1166.

——, and R. Zehr, 1981: Observational analysis of tropical cyclone formation. Part II: Comparison of non-developing versus non-developing Systems. *J. Atmos. Sci.*, **38**, 1132–1151.

Neelin, J. D., and I. M. Held, 1987: Modeling tropical convergence based on the moist static energy budget. *Mon. Wea. Rev.*, **115**, 3–12.

Nicholls, N., 1992: Recent performance of a method for forecasting Australian seasonal tropical cyclone activity. *Aust. Meteor. Mag.*, **40**, 105–110.

Roeckner, E., K. Arpe, L. Bengtsson, M. Christoph, M. Claussen, L. Dümenil, M. Esch, M. Giorgetta, U. Schlese, and U. Schulzweida, 1996: The atmospheric general circulation model ECHAM-4: Model description and simulation of present-day climate. Technical Report 218, Max-Planck Institute for Meteorology, 90 pp.

Rotunno, R., and K. Emanuel, 1987: An air-sea interaction theory for tropical cyclones. Part II: Evolutionary study using a non-hydrostatic axisymmetric model. *J. Atmos. Sci.*, **44**, 542–561.

Ryan, B. F., I. G. Watterson, and J. L. Evans, 1992: Tropical cyclone frequencies inferred from Gray's yearly genesis parameter: Validation of GCM tropical climate. *Geophys. Res. Lett.*, **19**, 1831–1834.

Thorncroft, C., and I. Pytharoulis, 2001: A dynamical approach to seasonal prediction of Atlantic tropical cyclone activity. *Wea. Forecasting*, **16**, 725–734.

Tsutsui, J. I., and A. Kasahara, 1996: Simulated tropical cyclones using the National Center for Atmospheric Research community climate model. *J. Geophys. Res.*, **101**, 15013–15032.

Vitart, F., and J. L. Anderson, 2001: Sensitivity of Atlantic tropical storm frequency to ENSO and interdecadal variability of SSTs in an ensemble of AGCM integrations. *J. Climate*, **14**, 533–545.

——, ——, and W. F. Stern, 1997: Simulation of interannual variability of tropical storm frequency in an ensemble of GCM integrations. *J. Climate*, **10**, 745–760.

——, ——, and ——, 1999: Impact of large-scale circulation on tropical storm frequency, intensity and location, simulated by an ensemble of GCM Integrations. *J. Climate*, **12**, 3237–3254.

——, and T. N. Stockdale, 2001: Seasonal forecasting of tropical storms using coupled GCM integrations. *Mon. Wea. Rev.*, **129**, 2521–2537.

Watterson, I. G., J. L. Evans, and B. F. Ryan, 1995: Seasonal and interannual variability of tropical cyclogenesis: Diagnostics from large-scale fields. *J. Climate*, **8**, 3042–3066.

Wu, G., and N. C. Lau, 1992: A GCM Simulation of the relationship between tropical storm formation and ENSO. *Mon. Wea. Rev.*, **120**, 958–977.

Zehr, R. M., 1992: Tropical cyclogenesis in the Western North Pacific. NOAA Technical Report NESDIS 61, NOAA, Washington, D.C., 181 pp.